Ultrasound renal stone diagnosis based on convolutional neural network and VGG16 features

Noor Hamzah Alkurdy[1,2], Hadeel K. Aljobouri[1], Zainab Kassim Wadi[3]

[1]Biomedical Engineering Department, College of Engineering, Al-Nahrain University, Baghdad, Iraq
[2]Diwaniyah Health Department, Diwaniyah General Teaching Hospital, Diwaniyah, Iraq
[3]Department of Radiology, Al-Imamain Al-Kadhimain Medical City Teaching Hospital, Baghdad, Iraq

Article Info

ABSTRACT

This paper deals with the classification of the kidneys for renal stones on ultrasound images. Convolutional neural network (CNN) and pre-trained CNN (VGG16) models are used to extract features from ultrasound images. Extreme gradient boosting (XGBoost) classifiers and random forests are used for classification. The features extracted from CNN and VGG16 are used to compare the performance of XGBoost and random forest. An image with normal and renal stones was classified. This work uses 630 real ultrasound images from Al-Diwaniyah General Teaching Hospital (a lithotripsy center) in Iraq. Classifier performance is evaluated using its accuracy, recall, and F1 score. With an accuracy of 99.47%, CNN-XGBoost is the most accurate model.
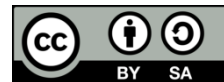
Corresponding Author:

Noor Hamzah Alkurdy
Biomedical Engineering Department, College of Engineering, Al-Nahrain University
Baghdad 10072, Iraq
Email: noor92_h@yahoo.com

1. INTRODUCTION

The kidneys' primary function is to keep the body in balance (homeostasis) by regulating fluid levels, regulating salt levels inside the body, and removing waste products from the blood. Mineral and salt deposits form inside the kidneys, causing renal stones. They can damage any part of the urinary tract, from the kidneys to the bladder. Minerals crystallize and bond together in concentrated urine, creating stones. This condition might be due to various factors, including diet, excess body weight, medical conditions, and specific nutritional supplements and drugs. Kidney stone illness affects people of all races. However, whites are the most affected, followed by Hispanics, Blacks, and Asians [1]. Kidney stones are considered a systemic issue associated with metabolic syndrome. The end-stage renal disease affects 2% to 3% of patients with combined nephrolithiasis and nephrocalcinosis [2]. Chronic kidney disease is more likely to occur in patients with a history of kidney stones [3]. When these calculi stones migrate through the ureter, they obstruct urine flow and cause intense discomfort known as renal colic. Urolithiasis can potentially cause morbidity and damage to the kidneys [4].

Ultrasonography, often known as ultrasound imaging, is a technique for visually inspecting interior tissues, muscles, and organs and performing quantitative analysis. Ultrasound is used to obtain measurements to diagnose disorders [5]. Ultrasound is performed as the first-line imaging examination of the abdomen and kidneys. Ultrasound is a safe, non-invasive, non-radioactive imaging modality [6]. Kidney stones seem brighter and more hyperechoic in ultrasound images because most ultrasound waves are reflected in the transducer [7], [8]. Recently, deep learning has become one of the most prominent subjects in artificial intelligence [9]. The architecture of the deep convolutional network leads to hierarchical feature extraction [10]. Convolutional

neural networks (CNNs) are a prominent area of study in image recognition research. CNN successfully processes raw pixel data for image categorization [11]. Correctly classifying medical images is critical for improving clinical care and therapy [12]. The deep CNN model is good at extracting features from images and classifying them. Deep learning algorithms extract essential features from data and have state-of-the-art accuracy, often surpassing that of individual intelligence [13]. CNN is the most widely used machine learning algorithm because it automatically discovers essential features without human intervention [14]. Visual geometry group-16 (VGG16) is a deep CNN (DCNN) [15].

Verma *et al.* [16] suggested a method for the detection of kidney stones or the absence of stones. Image enhancement was performed via the average filter, the Gaussian filter, and unsharp masking. Next, morphological procedures such as erosion and stretching, and entropy-based segmentation were applied to determine the region of interest. Principal component analysis (PCA) was used for feature extraction and reduction, and then k-nearest neighbor (k-NN) and support vector machine (SVM) classifiers were applied for classification. An examination of these two methods revealed that k-NN is superior to SVM. The accuracy of k-NN was 89%, while that of SVM was 84%. Sudharson and Kokil [17] introduced pre-trained DNN models, which were given three alternative datasets for extracting features and then classified using SVM. The model classifies the ultrasound images of the kidney into four categories: normal, cyst, stone, and tumor. When evaluated with high-quality images, the approach had a classification accuracy of 96.54% and 95.58% when noisy images were employed. Srivastava *et al.* [18] presented a common VGG16 model that was fine-tuned using its collection of ultrasound images. The model can tell if the ultrasound scans indicate an ovarian cyst or not and has an accuracy rate of 92.11%. Kokil and Sudharson [19] introduced an algorithm for automatically detecting and classifying kidney abnormalities. Pre-trained CNNs were utilized to extract features from the kidney ultrasound images. The extracted features were input into an SVM classifier to identify kidney abnormalities. The images were divided into three categories: normal, cystic, and stoned. A performance review was conducted, and 91.8% accuracy was achieved. The proposed models focus on features extracted by CNN and VGG16. Diagnose abnormalities in renal ultrasound images by using machine learning algorithms.

2. METHOD

The workflow of the suggested model is shown in Figure 1. This section is divided into two main sections: data collection and preprocessing steps. The details of these sections are introduced in the next paragraphs.
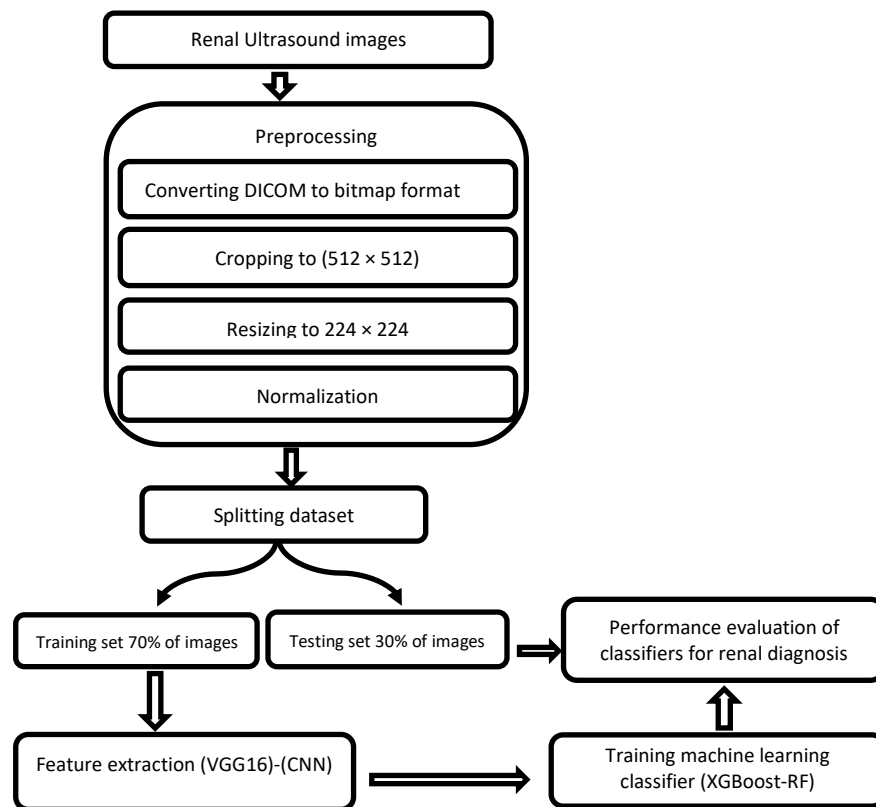

Figure 1. Proposed research

2.1. Data collection

Real images from Al-Diwaniyah General Teaching Hospital (Lithotripsy Center), Iraq, were collected using a Philips HD11 XE ultrasound system with image dimensions of 800×600 and digital imaging and communications in medicine (DICOM) format. The images were diagnosed by three radiologists and five urologists and classified into two groups: renal and normal renal stones. A total of 630 images-315 normal images and 315 stone images—were obtained.

2.2. Pre-processing

In medical imaging, data preparation is essential. In many cases, pre-processing steps are mandatory for meaningful data analysis [20]. Pre-processing is accomplished in this study using four steps, including image format, cropping, resizing, and normalization.

2.2.1. Image format

Renal ultrasound images were converted from DICOM to bitmap format. Then, the files were arranged, and the images were separated randomly into 70% (440 images for training) and 30% (190 for testing). Some images of normal kidneys and those containing stones are shown in Figures 2(a) and 2(b).
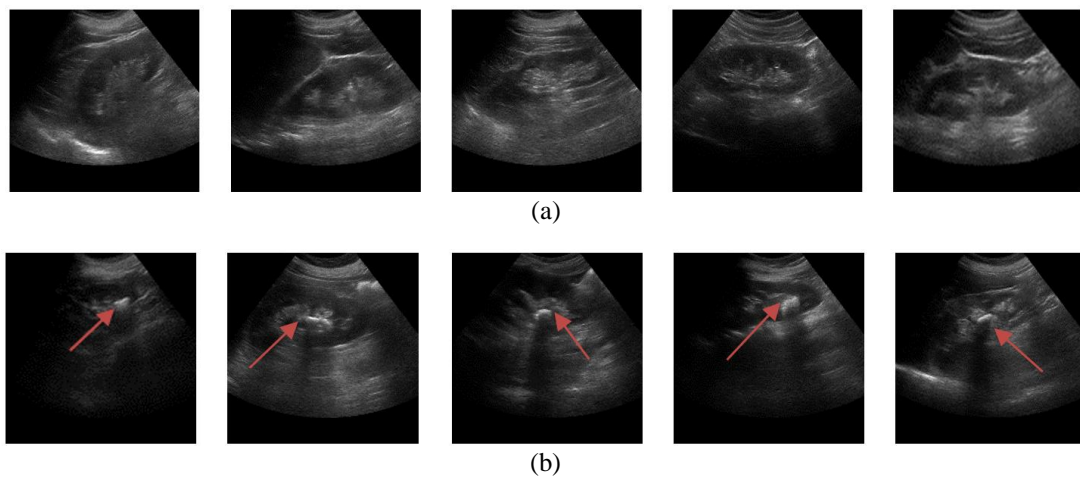

Figure 2. Renal ultrasound images (a) normal and (b) stone

2.2.2. Region of interest

Region of interest (ROI) is the process of cropping unwanted areas or unneeded information from ultrasound images, such as the patient's name and scanning details. It increases the classification process's speed and efficiency [21]. In the present work, a rectangular ROI is identified in the middle of images, and the images are cropped to a size of 512×512.

2.2.3. Resizing

Image size is adjusted without changing the amount of data in the image. Image resizing is used in image processing to increase and decrease the size of an image in pixel format [22]. In the present work, the images are scaled to a uniform size of 224×224.

2.2.4. Normalization

Normalization divides original data by 255 to ensure that all variance values are between 0 and 1. Normalization may be valuable for prediction [23]. It is beneficial for neural network-based classification methods [24].

2.3. Feature extraction

Feature extraction requires modifying the original features to create more significant features. Deep learning, especially when utilizing CNN, does not require a sophisticated way to extract features. CNN-trained datasets produce a wide range of results depending on the architecture and datasets [25]. More features correspond to increased difficulty in visualizing and interacting with the training dataset. For this research, CNN and VGG16 features were extracted from the convolution layer.

2.3.1. CNN

The CNN algorithm is a well-known and widely used algorithm that works by sending an image through a series of layers and then outputting a single class from a set of possible image classes [26]. It is capable of learning invariant local properties [26]. The advantages of CNN over other types of neural networks are its weight-sharing features, concurrent learning of the feature extraction layer and classification layers, and large-scale network implementation. CNN is a supervised learning method with several fully connected layers – including several hidden layers, an input layer, an output layer, and normalization layers [15] – that function similarly to individuals. In this study, the CNN consists of four convolution layers (conv2D), two MaxPooling2D, and four BatchNormalization layers. The fully connected layers (dense layer) are completely removed, as shown in Figure 3.
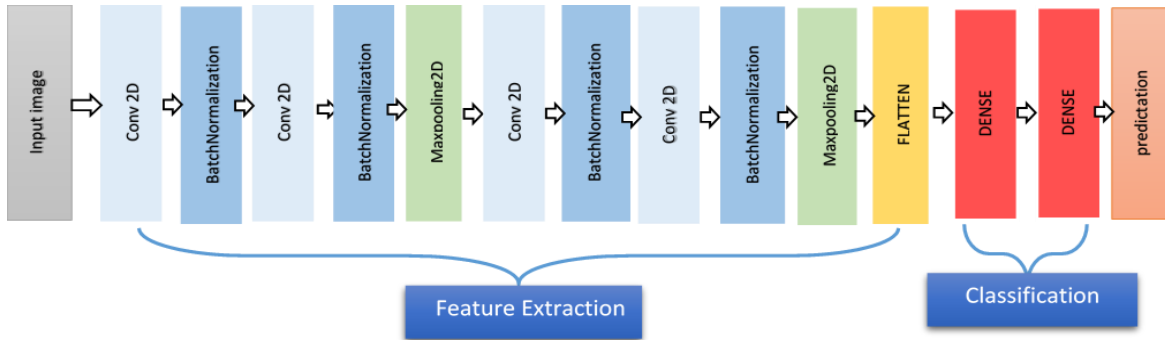

Figure 3. Structure of the CNN architecture

2.3.2. VGG16

VGG16-DCNN is assigned weights learned from the ImageNet database [12]. VGG16 has achieved high performance in feature extraction in medical imaging [9]. VGG-16 comprises 16 layers with configurable parameters (13 convolutional layers and three fully connected layers). In this research, the model is initially loaded to extract features with ImageNet-trained weights without fully connected layers (dense layers) of the classifier and by making loaded layers non-trainable. Afterward, features are extracted from VGG16 ImageNet weights to the classifier for prediction, as shown in Figure 4.
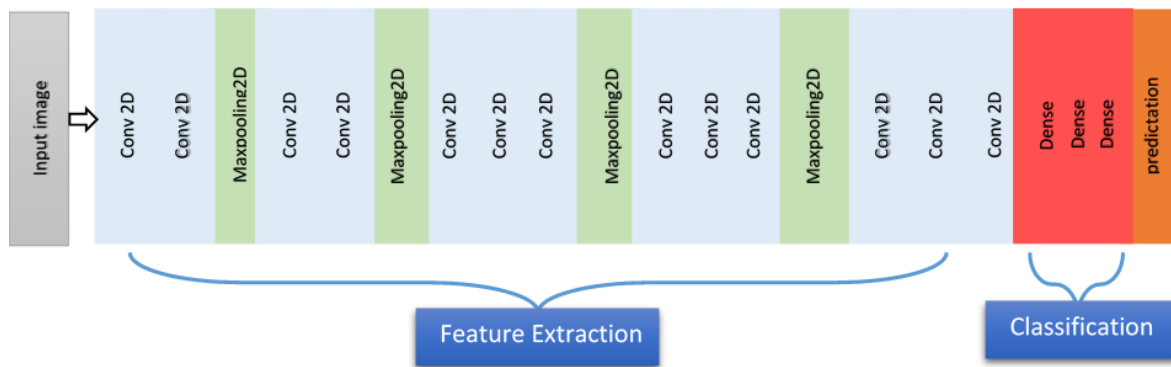

Figure 4. Structure of the VGG16 architecture

2.4. Classification algorithms

Image classification aims to lower the model's computational complexity, which is expected to rise if the input includes images. Image classification is a major part of the significant medical imaging concerns. The ultimate objective of medical imaging analysis is to classify images from several modalities to discriminate among different illness types of biomarkers [27]. Two machine learning techniques are used to diagnose ultrasound images: extreme gradient boosting (XGBoost) and random forest (RF).

2.4.1. XGBoost

XGboost is a decision tree boosting algorithm at its core. An ensemble learning procedure requires developing numerous models consecutively, with each new model trying to adjust for the deficiencies of the prior model [28]. The program first offers potential splitting points based on feature distribution percentiles. Then, the algorithm splits the continuous features into buckets specified by these option points, aggregates the statistics, and selects the best solution from among the suggestions based on the aggregated data [29]. Each iteration of the algorithm adds a new decision tree to the existing decision trees to increase the value of the desired function. The objective function of XGBoost is the sum of the loss function calculated over whole predictions and a regularization function for each prediction (K trees) [30].

$$Obj = \sum_{i=1}^{n} l(\mathcal{Y}_i, \hat{\mathcal{Y}}) + \sum_{k=1}^{K} \Omega(f_k) \tag{1}$$

where $l(\mathcal{Y}_i, \hat{\mathcal{Y}})$ is training loss measures how well the model fits on training data, Ω is regularization measures the complexity of trees, and K is number of trees. In this suggested approach, the XGBoost classifier makes accurate assumptions to obtain the best tree model.

2.4.2. Random forest

Random forest (RF) is a classification approach that uses ensemble learning and is widely used with large training datasets and many input variables. The decision tree is a popular classifier because of its fast execution speed [31]. The method's essence is the construction of several trees in randomly chosen subspaces of the feature set. Trees in various subspaces extend the classification in distinctive ways. Their overall classification can be incrementally improved [32]. RF's primary benefit is that it enhances forecast accuracy without raising computing expenses [33]. In the present research, the performance of the RF created with 50 trees trained with CNN and VGG16 features is investigated.

3. RESULTS AND DISCUSSION

Every experiment is performed using a Dell laptop with the following specifications: Intel® Core™ i7-6600U central processing unit (CPU) and 64-bit operating system. Python 3.9.7 is used. The installed software includes Anaconda Navigator, Spyder, and Python. The models are evaluated using a hold-out (70% to 30%) train–test split and K-fold cross-validation (K=5) for measuring the model's classification performance. A confusion matrix of the selected classifiers is utilized to evaluate the performance parameters, as shown in Figure 5.

The comparison shows that when CNN was used with XGBoost and RF classifiers, the classification accuracy was 99.47% and 98.94% for CNN-XGBoost and CNN-RF, respectively. These results were better than those of VGG16 when used with the same classifier. The accuracy of VGG16-RF and VGG16-XGBoost is 85.26% and 93.68%, respectively.

These models are evaluated using accuracy, precision, recall, and F1-score. Through the use of (2) to (5), the true negative (TN), true positive (TP), false negative (FN), and false positive (FP) values are calculated [34]. Accuracy is the ratio of the true predicted observation to the total observation, as determined by (2).

$$Accuracy = \frac{TP+TN}{TP+FP+FN+TN} \tag{2}$$

Precision is the weighted average of precision and recall, as determined by (3).

$$Precision = \frac{TP}{TP+FP} \tag{3}$$

Recall (sensitivity) is the ratio of the TP observations to the sum of TP and FN observations (all observations in the actual class) determined by (4).

$$Recall = \frac{TP}{TP+FN} \tag{4}$$

F1-score is the weighted average of precision and recall determined by (5).

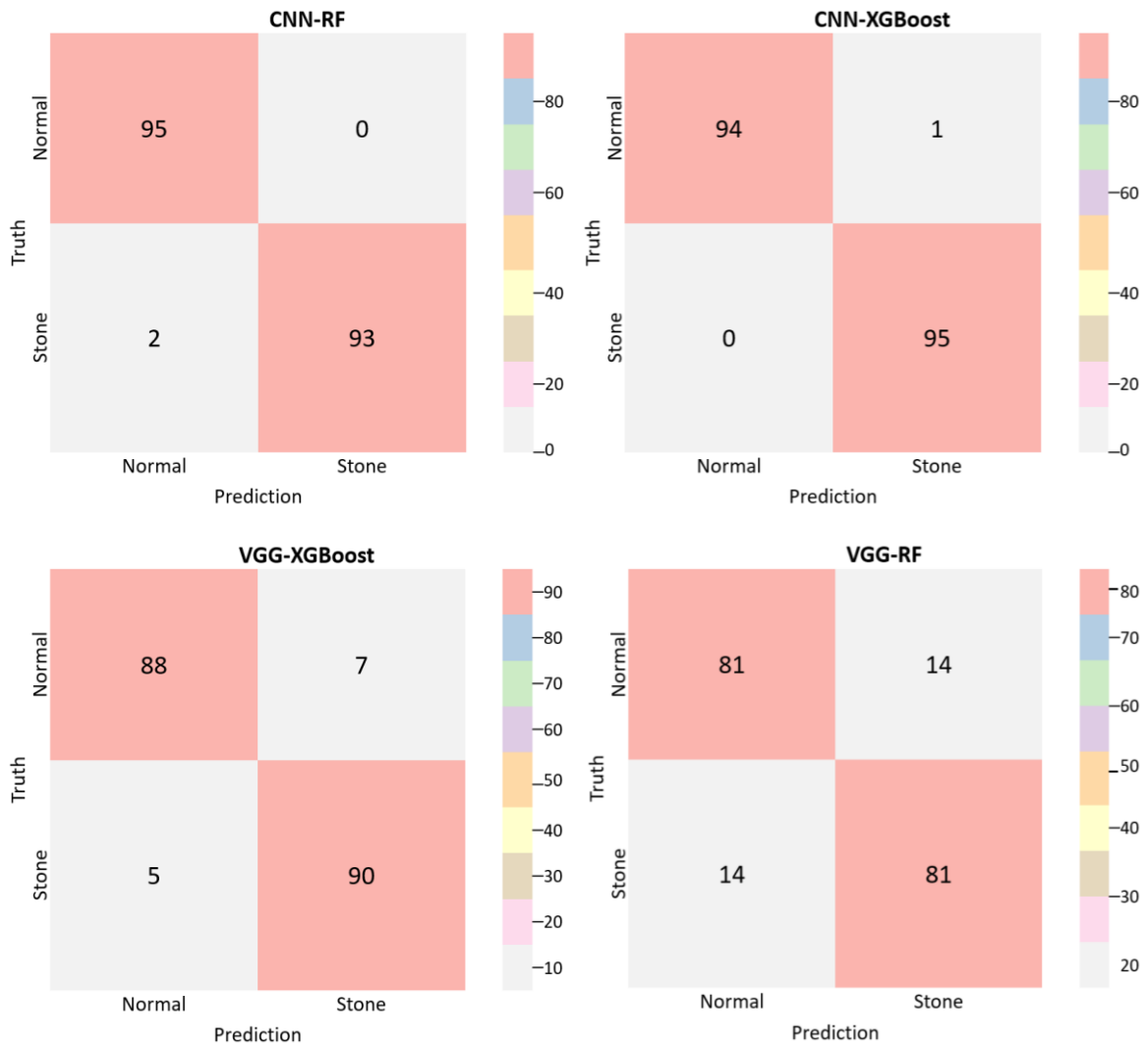$$F1\ score = \frac{2 \times (Recall \times Precision)}{Recall + Precision} \tag{5}$$

Figure 5. Confusion matrix of selected classifiers

A receiver operating characteristic (ROC) curve is a graph that shows the performance of a classification model over all classification thresholds. This curve demonstrates two parameters: TP rate and FP rate. The area under the (AUC) is measured to determine the ability of a classification system to distinguish between the classes. Figure 6 shows the charting of the ROC and AUC curves for the four models. For K-fold cross-validation, the data are divided into k parts. One part is set aside for validation for each iteration, and the other parts are combined and used to train the model. Finally, the average cross-validation performance across all iterations is used to evaluate the model. As a final stage in optimizing the model performance, K-fold validation (K = 5) was performed on the four models, as shown in Table 1. Table 2 shows the performance of various classifiers.

In this work, four models are proposed to detect abnormalities from renal ultrasound images using local datasets from Iraqi centers. Good performance (96.54% accuracy) was achieved on three variant datasets using the pre-trained DNN models and SVM for classification. The model classifies the ultrasound images of the kidney into four categories: normal, cyst, stone, and tumor [17]. The pre-trained off-the-shelf CNN was utilized to extract features from the kidney ultrasound images, and the SVM classifier was used to classify kidney images into normal, cystic, and stoned kidneys. A performance review was conducted, and 91.8% accuracy was achieved [19].

This paper proposes four models to classify renal stone ultrasound images. The proposed CNN-XGBoost and CNN-RF models have better classification accuracy than VGG16-XGBoost and VGG16-RF. The accuracy of CNN-XGBoost and CNN-RF, VGG16-XGBoost, and VGG16-RF is 99.47%, 98.94%, 93.68%, and 85.26%, respectively.
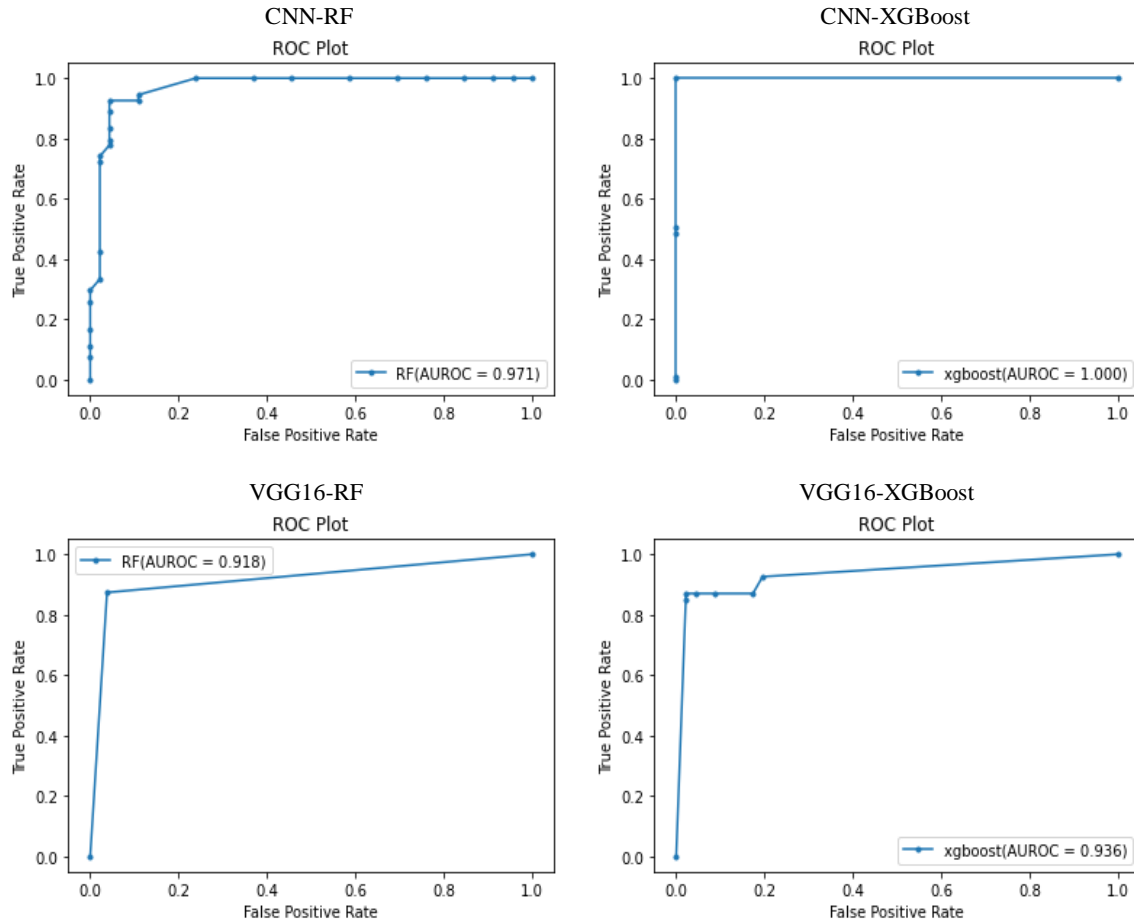
Figure 6. ROC and AUC curves for the four models

Table 1. Accuracy for the five-fold cross-validation for the four models

Model	K-Fold	Accuracy (%)	Mean accuracy (%)	Model	K-Fold	Accuracy %	Mean accuracy (%)
CNN-RF	1st -fold	1	0.984	VGG16-RF	1st -fold	0.886364	0.845
	2nd -fold	0.988636			2nd -fold	0.795455	
	3rd -fold	0.977273			3rd -fold	0.852273	
	4th -fold	0.965909			4th -fold	0.840909	
	5th -fold	0.988636			5th -fold	0.852273	
CNN-XGBoost	1st -fold	1	0.993	VGG16-XGBoost	1st -fold	0.965909	0.927
	2nd -fold	1			2nd -fold	0.886364	
	3rd -fold	1			3rd -fold	0.920455	
	4th -fold	0.965909			4th -fold	0.943182	
	5th -fold	1			5th -fold	0.920455	

Table 2. Performance of four models

Model	TP	TN	FP	FN	Accuracy	Precision	Recall	F1-score
CNN-RF	95	93	1	0	98.94	98	100	98
CNN-XGBOOST	94	95	0	2	99.47	100	97	98
VGG16-RF	81	81	14	14	85.26	92	94	92
VGG16-XGBOOST	88	90	7	5	93.68	86	86	86

Table 2 shows that the CNN-XGBoost model classifiers efficiently classify renal stones. The performance measure of the XGBoost and RF classifiers includes other parameters such as accuracy, recall, and F1-score. Five-fold cross-validation was performed to achieve objective, well-rounded assessments of metrics, resulting in more accurate models. The results of the five-fold cross-validation corroborated the earlier findings that the CNN-XGBoost model has the highest scores with 99.3% accuracy. Table 3 shows a comparison of our work to the literature review of recent studies.

Table 3. Summary of recent studies

No.	Author	Methodology	Type of Medical Image	Dataset	Accuracy
1	[16]	PCA + k-NN, SVM	Kidney ultrasound images	Stoned kidney, normal kidney	k-NN 89%, SVM 84%
2	[17]	Pre-trained DNN models + SVM	Kidney ultrasound images	Normal kidney, cystic kidney, stoned kidney, and tumor kidney	96.54%
3	[18]	VGG16	Ovarian ultrasound images	Ovarian cyst or not	92.11%
4	[19]	Pre-trained CNN + SVM	Kidney ultrasound images	Normal kidney, cystic kidney, and stoned kidney	91.8%
5	Proposed	CNN-XGBoost, CNN-RF, VGG16-XGBoost, VGG16-RF	Kidney ultrasound images	630 images for normal kidney, stoned kidney	CNN-XGBoost 98.94%, CNN-RF 99.47%, VGG16-XGBoost 93.68%, VGG16-RF 85.26%

4. CONCLUSION

Renal stone classification models were established using CNN and VGG16 for feature extraction and XGBoost and RF as classifiers. The proposed models indicated that the performance of feature extraction with CNN and the use of the classifier with XGBoost and RF is better than that of the pre-trained network VGG16. The features of XGBoost and RF are based on classification accuracy. The developed kidney stone classification models will serve as a supportive tool for radiologists, especially in Iraq. Given the acknowledged lack of clinical investigations and diagnostic capabilities, these models offer a possible solution to the loaded clinical situation in Iraq. In addition, these models can classify abnormalities of renal ultrasound images such as hydronephrosis (stones in the ureters), cysts, kidney failure, and tumors.

REFERENCES

[1] W. Shang et al., "History of kidney stones and risk of chronic kidney disease: a meta-analysis," PeerJ, vol. 5, Jan. 2017, doi: 10.7717/peerj.2907.

[2] T. Alelign and B. Petros, "Kidney stone disease: An update on current concepts," Advances in Urology, vol. 2018, pp. 1–12, 2018, doi: 10.1155/2018/3068365.

[3] V. K. Sigurjonsdottir, H. L. Runolfsdottir, O. S. Indridason, R. Palsson, and V. O. Edvardsson, "Impact of nephrolithiasis on kidney function," BMC Nephrology, vol. 16, no. 1, Dec. 2015, doi: 10.1186/s12882-015-0126-1.

[4] K. Mikawlrawng, S. Kumar, and Vandana, "Current scenario of urolithiasis and the use of medicinal plants as antiurolithiatic agents in Manipur (North East India): A review," International Journal of Herbal Medicine, vol. 2, no. 1, pp. 1–12, 2014.

[5] A. F. Ahmed, "Efficient approach for de-speckling medical ultrasound images using improved adaptive shock filter," Al-Nahrain Journal for Engineering Sciences (NJES), vol. 20, no. 5, pp. 1192–1197, 2017.

[6] J. A. Noble, "Ultrasound image segmentation and tissue characterization," Proceedings of the Institution of Mechanical Engineers, Part H: Journal of Engineering in Medicine, vol. 224, no. 2, pp. 307–316, Feb. 2010, doi: 10.1243/09544119JEIM604.

[7] V. E. Noble and D. F. M. Brown, "Renal ultrasound," Emergency Medicine Clinics of North America, vol. 22, no. 3, pp. 641–659, Aug. 2004, doi: 10.1016/j.emc.2004.04.014.

[8] C. Türk et al., "EAU guidelines on diagnosis and conservative management of urolithiasis," European Urology, vol. 69, no. 3, pp. 468–474, Mar. 2016, doi: 10.1016/j.eururo.2015.07.040.

[9] N. K. Chauhan and K. Singh, "A review on conventional machine learning vs deep learning," in 2018 International Conference on Computing, Power and Communication Technologies (GUCON), Sep. 2018, pp. 347–352, doi: 10.1109/GUCON.2018.8675097.

[10] N. Aloysius and M. Geetha, "A review on deep convolutional neural networks," in 2017 International Conference on Communication and Signal Processing (ICCSP), Apr. 2017, pp. 0588–0592, doi: 10.1109/ICCSP.2017.8286426.

[11] P. M. Cheng and H. S. Malhi, "Transfer learning with convolutional neural networks for classification of abdominal ultrasound images," Journal of Digital Imaging, vol. 30, no. 2, pp. 234–243, Apr. 2017, doi: 10.1007/s10278-016-9929-2.

[12] S. S. Yadav and S. M. Jadhav, "Deep convolutional neural network based medical image classification for disease diagnosis," Journal of Big Data, vol. 6, no. 1, Dec. 2019, doi: 10.1186/s40537-019-0276-2.

[13] D. Ciresan, U. Meier, and J. Schmidhuber, "Multi-column deep neural networks for image classification," in 2012 IEEE Conference on Computer Vision and Pattern Recognition, Jun. 2012, pp. 3642–3649, doi: 10.1109/CVPR.2012.6248110.

[14] K. Simonyan and A. Zisserman, "Very deep convolutional networks for large-scale image recognition," 3rd International Conference on Learning Representations, Sep. 2014.

[15] L. Alzubaidi et al., "Review of deep learning: concepts, CNN architectures, challenges, applications, future directions," Journal of Big Data, vol. 8, no. 1, Dec. 2021, doi: 10.1186/s40537-021-00444-8.

[16] J. Verma, M. Nath, P. Tripathi, and K. K. Saini, "Analysis and identification of kidney stone using Kth nearest neighbour (KNN) and support vector machine (SVM) classification techniques," Pattern Recognition and Image Analysis, vol. 27, no. 3, pp. 574–580, Jul. 2017, doi: 10.1134/S1054661817030294.

[17] S. Sudharson and P. Kokil, "An ensemble of deep neural networks for kidney ultrasound image classification," Computer Methods and Programs in Biomedicine, vol. 197, Dec. 2020, doi: 10.1016/j.cmpb.2020.105709.

[18] S. Srivastava, P. Kumar, V. Chaudhry, and A. Singh, "Detection of ovarian cyst in Ultrasound Images Using fine-tuned VGG-16 deep learning network," SN Computer Science, vol. 1, no. 2, Mar. 2020, doi: 10.1007/s42979-020-0109-6.

[19] P. Kokil and S. Sudharson, "Automatic detection of renal abnormalities by off-the-shelf CNN Features," IETE Journal of Education,

vol. 60, no. 1, pp. 14–23, Jan. 2019, doi: 10.1080/09747338.2019.1613936.

[20] A. Famili, W.-M. Shen, R. Weber, and E. Simoudis, "Data preprocessing and intelligent data analysis," *Intelligent Data Analysis*, vol. 1, no. 1, pp. 3–23, Jan. 1997, doi: 10.3233/IDA-1997-1102.

[21] W. M. Hafizah and E. Supriyanto, "Automatic region of interest generation for kidney ultrasound images," in *Proceedings of the 11th WSEAS international conference on Applied computer science*, 2011, pp. 70–75.

[22] S. Perumal and V. Thambusamy, "Preprocessing by contrast enhancement techniques for medical images," *International Journal of Pure and Applied Mathematics*, vol. 118, no. 18, pp. 3681–3688, 2018.

[23] S. G. K. Patro, P. P. Sahoo, I. Panda, and K. K. Sahu, "Technical analysis on financial forecasting," *Prepr. arXiv1503.03011*, 2015,

[24] L. Al Shalabi, Z. Shaaban, and B. Kasasbeh, "Data mining: A preprocessing engine," *Journal of Computer Science*, vol. 2, no. 9, pp. 735–739, Sep. 2006, doi: 10.3844/jcssp.2006.735.739.

[25] A. B. Perdana and A. Prahara, "Face recognition using light-convolutional neural networks based on modified Vgg16 model," in *2019 International Conference of Computer Science and Information Technology (ICoSNIKOM)*, Nov. 2019, pp. 1–4, doi: 10.1109/ICoSNIKOM48755.2019.9111481.

[26] Y. Saleh and G. F. Issa, "Arabic sign language recognition through deep neural networks fine-tuning," *International Journal of Online and Biomedical Engineering (iJOE)*, vol. 16, no. 05, pp. 71–83, May 2020, doi: 10.3991/ijoe.v16i05.13087.

[27] Y. Song *et al.*, "Large margin local estimate with applications to medical image classification," *IEEE Transactions on Medical Imaging*, vol. 34, no. 6, pp. 1362–1377, Jun. 2015, doi: 10.1109/TMI.2015.2393954.

[28] R. Mitchell and E. Frank, "Accelerating the XGBoost algorithm using GPU computing," *PeerJ Computer Science*, vol. 3, Jul. 2017, doi: 10.7717/peerj-cs.127.

[29] T. Chen and C. Guestrin, "XGBoost: A scalable tree boosting system," in *Proceedings of the 22nd ACM SIGKDD International Conference on Knowledge Discovery and Data Mining*, Aug. 2016, pp. 785–794, doi: 10.1145/2939672.2939785.

[30] Z. E. Aydin and Z. K. Ozturk, "Performance analysis of XGBoost classifier with missing data," *Manchester Journal of Artificial Intelligence and Applied Sciences (MJAIAS)*, vol. 2, no. 2, pp. 1–5, 2021.

[31] D. Gao, Y.-X. Zhang, and Y.-H. Zhao, "Random forest algorithm for classification of multiwavelength data," *Research in Astronomy and Astrophysics*, vol. 9, no. 2, pp. 220–226, Feb. 2009, doi: 10.1088/1674-4527/9/2/011.

[32] Tin Kam Ho, "Random decision forests," in *Proceedings of 3rd International Conference on Document Analysis and Recognition*, 1995, vol. 1, pp. 278–282, doi: 10.1109/ICDAR.1995.598994.

[33] H. EL Hamdaoui, S. Boujraf, N. E. H. Chaoui, B. Alami, and M. Maaroufi, "Improving heart disease prediction using random forest and AdaBoost algorithms," *International Journal of Online and Biomedical Engineering (iJOE)*, vol. 17, no. 11, pp. 60–75, Nov. 2021, doi: 10.3991/ijoe.v17i11.24781.

[34] I. D. Irawati, I. Andrea Larasaty, and S. Hadiyoso, "Comparison of convolution neural network architecture for colon cancer classification," *International Journal of Online and Biomedical Engineering (iJOE)*, vol. 18, no. 03, pp. 164–172, Mar. 2022, doi: 10.3991/ijoe.v18i03.27777.

BIOGRAPHIES OF AUTHORS

Noor Hamzah Alkurdy obtained her B.S. in biomedical engineering from Al-Khwarizmi Engineering College, University of Baghdad, Baghdad, Iraq, in 2015. She is currently pursuing her M.Sc. in biomedical engineering at Al-Nahrain University. She has worked as a biomedical engineer at the Al-Diwaniyah General Teaching Hospital. Her research interests include biological image processing and medical applications of artificial intelligence. She can be contacted at noor92_h@yahoo.com.

Hadeel K. Aljobouri received her B.S. in biomedical engineering from the University of Baghdad in 2000. She received her M.Sc. in medical engineering from Al-Nahrain University, Baghdad, Iraq, in 2004, and her Ph.D. at the Electrical and Electronics Engineering Department, Graduate School of Natural Science, Ankara Yıldırım Beyazıt University in Turkey. She worked as an assistant professor at the Biomedical Engineering Department at Al-Nahrain University in Iraq. Her research interests are biomedical signal processing, medical imaging, data mining, clustering techniques, and machine learning. She has many publications in the field of biomedical engineering. She can be contacted at hadeel_bme77@yahoo.com.

Zainab Kassim Wadi received her MBChB from the College of Medicine at Al-Nahrain University in 2006. She received her FIBMS (Radiology) from the Iraqi Board for Medical Specializations in 2017, in Baghdad, Iraq. She is working as a senior radiologist at Al-Imamain Al-Kadhimain Medical City Teaching Hospital and is one of the founders of the Iraqi Society of Radiologists and Medical Imaging. She worked as a trainer for Iraqi board students in 2022. She can be contacted at zainabsamiradiology@gmail.com.